Increasing the Nuclearity of Magnetic Polyoxometalates. Syntheses, Structures, and Magnetic Properties of Salts of the Heteropoly Complexes $[Ni_3(H_2O)_3(PW_{10}O_{39})H_2O]^{7-}$, $[Ni_4(H_2O)_2(PW_9O_{34})_2]^{10-}$, and $[Ni_9(OH)_3(H_2O)_6(HPO_4)_2(PW_9O_{34})_3]^{16-}$

Juan M. Clemente-Juan, Eugenio Coronado,* José R. Galán-Mascarós, and Carlos J. Gómez-García

Departamento de Química Inorgánica, Universidad de Valencia, Dr. Moliner 50, E-46100 Burjasot, Spain

Received July 9, 1998

The rational synthesis and the structural and magnetic characterization of three different nickel clusters encapsulated in Keggin trivacant fragments are presented. The three complexes show how it is possible to increase the nuclearity of the clusters (from 3 and 4 to 9) by slightly changing the synthetic conditions. These three anionic clusters crystallize as mixed salts of K^+ and Na^+. The trimeric complex $[Ni_3(H_2O)_3PW_{10}O_{39}H_2O]^{7-}$ (**Ni$_3$**) crystallizes in the triclinic space group $P\bar{1}$ (a = 10.896(6) Å, b = 12.869(5) Å, c = 20.373(6) Å, α = 94.67(6)°, β = 101.12(8)°, γ = 110.72(8)°, Z = 2) and presents a ferromagnetic triangular cluster. The tetranuclear complex $[Ni_4(H_2O)_2(PW_9O_{34})_2]^{10-}$ (**Ni$_4$**) crystallizes in the monoclinic space group $P2_1/n$ (a = 11.824(5) Å, b = 16.551(6) Å, c = 21.074(5) Å, β = 100.38(2)°, Z = 2) and presents a ferromagnetic rhomb-like cluster. The nonanuclear complex $[Ni_9(OH)_3(H_2O)_6(HPO_4)_2(PW_9O_{34})_3]^{16-}$ (**Ni$_9$**) crystallizes in the monoclinic space group $P2_1/c$ (a = 30.589(10) Å, b = 12.521(6) Å, c = 39.456(11) Å, β = 102.49(3)°, Z = 4) and presents an antiferromagnetic triangle formed by three ferromagnetic triangular clusters. The magnetic properties of the three complexes are discussed on the basis of their topologies and fitted according to an isotropic exchange model (for the three clusters) and including the local anisotropy of each center (for the **Ni$_3$** and **Ni$_4$** clusters).

Introduction

Magnetic clusters with increasing numbers of exchange coupled centers is an area of current interest in molecular magnetism.[1] A class of compounds that provide ideal examples to study this kind of magnetic systems are the polyoxometalates of W and Mo.[2] Their suitability in this area is based on the following considerations: (1) they can coordinate groups of paramagnetic ions at specific sites of their structures; (2) thanks to the rigidity and size of the diamagnetic heteropoly framework they impose the geometry of the magnetic cluster keeping it well isolated from the neighboring clusters; (3) their chemistry allows the assembly of stable anion fragments into larger clusters; and (4) they can be reversibly reduced to mixed-valence species (heteropoly "blues" and "browns") by addition of various specific numbers of electrons, which are delocalized over a significantly large number of atoms of the heteropoly framework, retaining the gross structures of the oxidized anions.

Taking advantage of points 1−3, magnetic clusters with unusual geometries and highly symmetrical topologies have been obtained, for which the nuclearity can be increased with ease while their relevant structural features are maintained unchanged, and consequently the sign and magnitude of the exchange parameters. On the other hand point 4 allowed us to obtain large mixed valence clusters of W and Mo in which localized and delocalized electrons can coexist and interact,[3] thus providing the opportunity to investigate the interplay of electron transfer and magnetic interactions at the molecular level.[4] In this context the mixed-valence magnetic polyoxovanadates also play a relevant role.[5]

We present in this paper three novel polyoxometalate complexes of Ni(II) that illustrate in particular point 3: $[Ni_3(H_2O)_3(PW_{10}O_{39})H_2O]^{7-}$ (**Ni$_3$**), $[Ni_4(H_2O)_2(PW_9O_{34})_2]^{10-}$ (**Ni$_4$**), and $[Ni_9(OH)_3(H_2O)_6(HPO_4)_2(PW_9O_{34})_3]^{16-}$ (**Ni$_9$**). These complexes are based on the tungstophosphate ligand $[PW_9O_{34}]^{9-}$ (B isomer), which is the trivacant lacunary fragment that results from the removal of a triad of tungsten sites from the Keggin anion $[PW_{12}O_{40}]^{3-}$. The ability of this anion to act as ligand incorporating magnetic clusters into the structure is well-known. For example, an extensive series of tetranuclear sandwich complexes $[M_4(H_2O)_2(PW_9O_{34})_2]^{10-}$ (in short M_4) is known with

* Corresponding author. E-mail: eugenio.coronado@uv.es.

(1) Gatteschi, D.; Caneschi, A.; Pardi, L.; Sessoli, R. *Science* **1994**, *265*, 1054.

(2) (a) Coronado, E.; Gómez-García, C. J. *Comments Inorg. Chem.* **1995**, *17*, 255. (b) Coronado, E.; Gómez-García, C. J. In *Polyoxometalates: From Platonic Solids to Anti-retroviral activity*; Pope, M. T., Muller, A., Eds.; Kluwer Academic Publishers: Dordrecht, The Netherlands, 1994; p 233. (c) Clemente-Juan, J. M.; Clemente-León, M.; Coronado, E.; Galán-Mascarós, J. R.; Giménez-Saiz, C.; Gómez-García, C. J. *C. R. Acad. Sci. Paris, Ser. IIC*, **1998**, 305.

(3) (a) Casañ-Pastor, N.; Baker, L. C. W. *J. Am. Chem. Soc.* **1992**, *114*, 10384. (b) Casañ-Pastor, N.; Baker, L. C. W. In *Polyoxometalates: From Platonic Solids to Anti-retroviral activity*; Pope, M. T., Muller, A., Eds.; Kluwer Academic Publishers: Dordrecht, The Netherlands, 1994; p 203.

(4) (a) Borrás-Almenar, J. J.; Clemente, J. M.; Coronado, E.; Tsukerblat, B. S. *Chem. Phys.* **1995**, *195*, 1. (b) Borrás-Almenar, J. J.; Clemente, J. M.; Coronado, E.; Tsukerblat, B. S. *Chem. Phys.* **1995**, *195*, 17. (c) Borshch, S. A. *Inorg. Chem.* **1998**, *37*, 3116.

(5) Müller, A.; Peters, F.; Pope, M. T.; Gatteschi, D. *Chem. Rev.* **1998**, *98*, 239.

(6) (a) Weakley, T. J. R.; Evans, H. T.; Showell, J. S.; Tourné, G. F.; Tourné, C. M. *J. Chem. Soc. Chem. Commun.* **1973**, 139. (b) Evans, H. T.; Tourné, G. F.; Tourné, C. M.; Weakly, T. J. R.; *J. Chem. Soc., Dalton Trans.* **1986**, 2699. (c) Finke, R. G.; Droege, M. W.; Domaille, P. J. *Inorg. Chem.* **1987**, *26*, 3886. (d) Weakley, T. J. R.; Finke, R. G. *Inorg. Chem.* **1990**, *29*, 1235. (e) Gómez-García, C.; Coronado, E.; Gómez-Romero, P.; Casañ-Pastor, N. *Inorg. Chem.* **1993**, *32*, 3378.

10.1021/ic9807902 CCC: $18.00
Published on Web 12/17/1998

various divalent metal ions (M^{II} = Mn, Fe, Co, Cu, Zn).[2,6] The mixed-valence $Mn^{II}Mn^{III}$ tetranuclear analogue,[7] a mixed Fe^{III}_2-Cu^{II}_2 complex,[8] and the Fe^{III} complex[9] of this structural type are also known. The larger anion $[Co_9(OH)_3(H_2O)_6(HPO_4)_2(PW_9O_{34})_3]^{16-}$ (**Co_9**), which contains a nonanuclear Co(II) cluster, was also identified by Weakley[10] as a byproduct (ca. 5%) in the preparation of $[Co_4(H_2O)_2(PW_9O_{34})_2]^{10-}$. This author also reported the gross structural features of this giant polyoxoanion.[11] During the last 10 years we have been interested in the magneto-structural properties of these kinds of polyoxometalate complexes[6e,12,13] and in those complexes derived from the related ligand $[P_2W_{15}O_{56}]^{12-}$,[12b,14] A variety of techniques, including not only the classical ones (magnetic susceptibility, magnetization and EPR) but also inelastic neutron scattering (INS) spectroscopy,[15] have been used to obtain information about the energy levels and exchange interactions in these clusters.

Experimental Section

Syntheses. $K_6Na[Ni_3(H_2O)_3PW_{10}O_{39}H_2O]\cdot12H_2O$ (Ni$_3$). A solution of 2.49 g (10 mmol) of $Ni(OOC-CH_3)_2\cdot4H_2O$ in 50 mL of water was added to 100 mL of an aqueous solution containing 9.87 g (33 mmol) of $Na_2WO_4\cdot2H_2O$ and 0.425 g (3 mmol) of Na_2HPO_4 with pH adjusted to 6.5 with acetic acid. The resulting yellow solution (pH = 6.3) was refluxed for 2 h and hot filtered, and then 4 g of $K(OOC-CH_3)$ was added to the filtrate while hot. After several days small pale green needle-shaped crystals of the desired product were isolated by filtration and dried under vacuum (yield = 5.5 g; 51%). Anal. Calcd for $K_6Na[Ni_3(H_2O)_3PW_{10}O_{39}H_2O]\cdot12H_2O$: Ni, 5.48; W, 57.18; K, 7.30; Na, 0.72; H_2O, 6.72. Found: Ni, 5.52; W, 57.16; K, 7.28; Na, 0.70; H_2O, 6.73.

$K_6Na_4[Ni_4(H_2O)_2(PW_9O_{34})_2]\cdot24H_2O$ (Ni$_4$). A solution of 5.53 g (22 mmol) of $Ni(OOC-CH_3)_2\cdot4H_2O$ in 50 mL of water was added to 100 mL of an aqueous solution containing 33 g (100 mmol) of $Na_2WO_4\cdot2H_2O$ and 1.57 g (11 mmol) of Na_2HPO_4 with pH adjusted to 7.1 with acetic acid. The resulting yellow solution (pH = 6.9) was refluxed for 2 h and hot filtered, and then 4 g of $K(OOC-CH_3)$ was added to the filtrate while hot. After several hours a mixture of chunky small yellow crystals and powder of the desired product is obtained (yield = 19.4 g, 64%). Anal. Calcd for $K_6Na_4[Ni_4(H_2O)_2(PW_9O_{34})_2]\cdot24H_2O$: Ni, 4.31; W, 60.69; K, 4.30; Na, 1.68; H_2O, 7.27. Found: Ni, 4.24; W, 60.75; K, 4.20; Na, 1.80; H_2O, 7.21.

$K_5Na_{11}[Ni_9(OH)_3(H_2O)_6(HPO_4)_2(PW_9O_{34})_3]\cdot52H_2O$ (Ni$_9$). The pH of an aqueous solution of 16.5 g (50 mmol) of $Na_2WO_4\cdot2H_2O$ and 0.78 g (5.5 mmol) of Na_2HPO_4 was adjusted to 7.9 with acetic acid. A solution containing 4.1 g (16 mmol) of $Ni(OOC-CH_3)_2\cdot4H_2O$ in 30 mL of H_2O was added to the first one. The resulting green solution (pH = 7.5) was refluxed for 2 h. A 4 g amount of Na_2HPO_4 was added, and the solution was refluxed again for 9 h and hot filtered. After adding 5 g of solid $K(OOC-CH_3)$, the resulting solution was allowed to cool at room temperature. After several hours small green needle-shaped crystals of the desired product were isolated by filtration and dried under vacuum. This product was recrystallized from hot water to obtain good-quality single crystals suitable for X-ray diffraction analysis (yield = 4.1 g; 27%). Anal. Calcd for $K_5Na_{11}[Ni_9(OH)_3(H_2O)_6(HPO_4)_2(PW_9O_{34})_3]\cdot52H_2O$: Ni, 5.94; W, 55.84; K, 2.20; Na, 2.83; H_2O, 10.54. Found: Ni, 6.30; W, 55.91; K, 2.43; Na, 2.60; H_2O, 10.54.

Table 1. Crystal Data and Structure Refinement Data for **Ni$_3$**, **Ni$_4$**, and **Ni$_9$**

	Ni$_3$	**Ni$_4$**	**Ni$_9$**
empirical formula	$H_{32}K_6NaNi_3O_{55}PW_{10}$	$H_{52}K_6Na_4Ni_4O_{94}P_2W_{18}$	$H_{121}K_5Na_{11}Ni_9O_{171}P_5W_{27}$
a	10.896(6) Å	11.824(5) Å	30.589(10) Å
b	12.869(5) Å	16.551(6) Å	12.521(6) Å
c	20.373(6) Å	21.074(5) Å	39.456(11) Å
α	94.67(6)°	90.0°	90.0°
β	101.12(8)°	100.38(2)°	102.49(3)°
γ	110.72(8)°	90.0°	90.0°
V	2586(1) Å^3	4056(2) Å^3	14754(10) Å^3
Z	2	2	4
fw	3215.43	5485.02	8467.01
space group	$P\bar{1}$ (No. 2)	$P2_1/n$ (No. 14)	$P2_1/c$ (No. 14)
T	20 °C	20 °C	20 °C
λ	0.710 73 Å	0.710 69 Å	0.710 69 Å
ρ_{calcd}	4.2128 g cm^{-3}	4.490 g cm^{-3}	3.836 g cm^{-3}
μ	243.36 cm^{-1}	26.808 cm^{-1}	22.527 cm^{-1}
R (F_o)[a]	0.0480	0.0509	0.0756
R_w (F_o)	0.0630[b]	0.1492[c]	0.2001[d]

[a] $R = \sum(F_o - F_c/\sum F_o$.7 [b] $R_w = [\sum\omega(F_o - F_c)^2/\sum\omega(F_o)^2]^{1/2}$. $\omega = 4F_o^2/[\sigma^2(I) + (0.07(F_o)^2)^2]$. [c] $R_w = [\sum[\omega(F_o^2 - F_c^2)^2]/\sum[\omega(F_o^2)^2]]^{1/2}$; $\omega = 1/[\sigma^2(F_o^2) + (0.0711P)^2 + 489.0567P]$, where $P = (F_o^2 + 2F_c^2)/3$. [d] $R_w = [\sum[\omega(F_o^2 - F_c^2)^2]/\sum[\omega(F_o^2)^2]]^{1/2}$; $\omega = 1/[\sigma^2(F_o^2) + (0.1374P)^2 + 1089.2701P]$, where $P = (F_o^2 + 2F_c^2)/3$.

X-ray Data Collection and Structure Refinement. Structure of **Ni$_3$** was already communicated.[16] A yellow prismatic crystal of **Ni$_4$** and a green needle-shaped crystal of **Ni$_9$** were taken directly from their mother liquor and mounted on a CAD4 Enraf-Nonius diffractometer. Crystals of **Ni$_9$** decompose after several hours due to solvent loss, and so this crystal was sealed in a Lindemann glass capillary before X-rays analysis. Preliminary examinations and data collection were performed with Mo Kα radiation. Unit cell parameters and orientation matrix were determined by a least-squares refinement of the setting angles of 25 independent reflections for both crystals. Data collection were performed with the ω scan technique, and three standard reflections were measured every 2 h and showed no significant decay. Lorentz, polarization, and semiempirical absorption corrections (ψ scan method) were applied to the intensity data. Selected experimental parameters and crystal data are reported in Table 1. The space group was determined to be $P2_1/n$ for **Ni$_4$** (the same space group is found for the analogous Co_4 and Zn_4 anions, but the unit cell is slightly different in this case) and $P2_1/c$ for **Ni$_9$**. The overall structure of **Ni$_9$** is very different to the already reported for the Rubidium salt of the Co_9 anionic analogue[10] (hexagonal space group $P6_3/m$, with anion crystallographic symmetry $3/m-C_{3h}$). In our case the whole anion is present in the asymmetric unit with no local symmetry. All calculations were performed in a SPARC Station 20 (Sun Microsystems). Both structures were solved by direct methods using the SIR92[17] program and refined on F^2 using the SHELXL-93 program (G. M. Sheldrick, University of Göttingen, 1993). Atomic parameters are given in Tables 2 and 3. In the structures solutions the atoms belonging to the anion were readily obtained, and afterward successive Fourier differences showed several peaks that were assigned

(7) Zhang, X. Y.; Jameson, G. B.; O'Connor, C. J.; Pope, M. T. *Polyhedron* **1996**, *15*, 917.
(8) Wasfi, S. H.; Rheingold, A. L.; Kokoszka, G. F.; Goldstein, A. S. *Inorg. Chem.* **1987**, *26*, 2934
(9) Zhang, X. Y.; Chen, Q.; Duncan, D. C.; Lachiotte, R. J.; Hill, C. L. *Inorg. Chem.* **1997**, *36*, 4381.
(10) Weakley, T. J. R. *J. Chem. Soc. Chem. Commun.* **1984**, 1406.
(11) The poor quality of the crystals, which diffracted with a very marked decline in scattering intensity with increasing *q* and the many disordered lattice water molecules, prevented an accurate determination of the structure.
(12) (a) Gómez-García, C. J.; Casañ-Pastor, N.; Coronado, E.; Baker, L. C. W.; Pourroy, G. *J. Appl. Phys.* **1990**, *67*, 5995. (b) Gómez-García, C. J.; Coronado, E.; Borrás-Almenar, J. J. *Inorg. Chem.* **1992**, *31*, 1667. (c) Casañ-Pastor, N.; Bas, J.; Coronado, E.; Pourroy, G.; Baker, L. C. W. *J. Am. Chem. Soc.* **1992**, *114*, 10380.
(13) (a) Galán-Mascarós, J. R.; Gómez-García, C. J.; Borrás-Almenar, J. J.; Coronado, E. *Adv. Mater.* **1994**, *6*, 221. (b) Borrás-Almenar, J. J.; Coronado, E.; Gómez-García, C. J.; Galán-Mascarós, J. R. *J. Magn. Magn. Mater.* **1995**, *140−144*, 1809.
(14) Gómez-García, C. J.; Borrás-Almenar, J. J.; Coronado, E.; Ouahab, L. *Inorg. Chem.* **1994**, *33*, 4016.
(15) (a) Gómez-García, C. J.; Coronado, E.; Borrás-Almenar, J. J.; Aebersold, M.; Güdel, H. U.: Mutka, H. *Physica B* **1992**, *180−181*, 238. (b) Clemente, J. M.; Andres, H.; Coronado, E.; Güdel, H. U.; Büttne, H.; Kearly, G. *Inorg. Chem.* **1997**, *36*, 2244.
(16) Gómez-García, C. J.; Coronado, E.; Ouahab, L. *Angew. Chem., Int. Ed. Engl.* **1992**, *31*, 649.
(17) Altomare, A.; Cascarano, G.; Giacovazzo, C.; Guagliardi, A. *J. Appl. Crystallogr.* **1994**, *27*, 1045.

Table 2. Atom Coordinates and Thermal Isotropic or Equivalent Isotropic Parameters for $H_{52}K_6Na_4Ni_4O_{94}P_2W_{18}$ (**Ni$_4$**)[a]

atom	*x*	*y*	*z*	*U* (Å^2)	atom	*x*	*y*	*z*	*U* (Å^2)
W1	0.49134(8)	0.27868(6)	0.18026(5)	0.0061(2)*	O21	0.6853(14)	0.1297(10)	0.0996(8)	0.007(3)
W2	0.66780(8)	0.36257(6)	0.06668(5)	0.0079(2)*	O22	0.364(2)	0.2906(12)	0.0003(9)	0.019(4)
W3	0.79495(8)	0.21294(6)	0.19003(5)	0.0062(2)*	O23	0.6069(14)	0.3063(10)	−0.0937(8)	0.010(3)
W4	0.29131(8)	0.21664(6)	0.04884(5)	0.0060(2)*	O24	0.8393(13)	0.1865(10)	0.0142(8)	0.006(3)
W5	0.46259(8)	0.30231(6)	−0.06349(5)	0.0072(2)*	O25	0.8454(14)	0.0215(10)	0.1364(8)	0.007(3)
W6	0.73870(8)	0.24383(6)	−0.05425(5)	0.0076(2)*	O26	0.5682(13)	0.0537(10)	0.1906(8)	0.006(3)
W7	0.86764(8)	0.09631(6)	0.06669(5)	0.0063(2)*	O27	0.2792(14)	0.1424(10)	0.1200(8)	0.009(4)
W8	0.70989(8)	0.01477(6)	0.17049(4)	0.0050(2)*	O28	0.5352(13)	0.0845(10)	0.0047(8)	0.004(3)
W9	0.40896(8)	0.07956(6)	0.16247(4)	0.0045(2)*	O29	0.292(2)	0.1337(11)	−0.0039(8)	0.011(4)
Ni1	0.3690(2)	0.0269(2)	−0.00391(14)	0.0041(6)*	O30	0.4324(14)	0.2045(10)	−0.0947(8)	0.010(4)
Ni2	0.5196(3)	0.0996(2)	−0.09740(14)	0.0048(6)*	O31	0.6743(13)	0.1532(10)	−0.0844(8)	0.005(3)
P	0.5765(5)	0.1535(4)	0.0523(3)	0.0030(11)*	O32	0.781(2)	0.0316(11)	0.0115(8)	0.012(4)
O1	0.477(2)	0.3473(12)	0.2380(10)	0.021(4)	O33	0.6314(14)	−0.0376(10)	0.1006(8)	0.008(3)
O2	0.713(2)	0.4572(12)	0.0919(10)	0.019(4)	O34	0.4014(14)	0.0120(10)	0.0947(8)	0.011(4)
O3	0.881(2)	0.2586(12)	0.2524(9)	0.017(4)	O35	0.5134(14)	0.1175(10)	−0.1941(8)	0.010(3)
O4	0.150(2)	0.2493(11)	0.0293(9)	0.016(4)	K1	0.0703(6)	0.9968(4)	0.6827(3)	0.0250(14)*
O5	0.3798(14)	0.3644(11)	−0.1184(8)	0.012(4)	K2	0.6356(7)	0.1339(5)	0.3186(4)	0.035(2)*
O6	0.835(2)	0.2619(12)	−0.1046(9)	0.017(4)	K3	0.0591(7)	0.1247(5)	0.9366(4)	0.040(2)*
O7	1.005(2)	0.0715(12)	0.0576(9)	0.019(4)	Na1	0.8069(12)	0.0577(8)	0.7615(7)	0.037(3)*
O8	0.7461(14)	−0.0583(10)	0.2274(8)	0.007(3)	Na2	0.462(2)	−0.0199(14)	0.4010(11)	0.085(7)*
O9	0.350(2)	0.0275(11)	0.2164(9)	0.014(4)	O1W	0.134(2)	0.1924(14)	0.1973(11)	0.030(5)
O10	0.556(2)	0.3421(11)	0.1204(9)	0.014(4)	O2W	0.149(2)	−0.0553(13)	0.1223(10)	0.028(5)
O11	0.6466(13)	0.2404(9)	0.2072(7)	0.004(3)	O3W	0.283(2)	−0.1792(14)	0.2248(11)	0.029(5)
O12	0.7655(14)	0.2983(10)	0.1284(8)	0.009(3)	O4W	0.187(2)	0.1994(13)	0.8546(10)	0.030(5)
O13	0.3495(14)	0.2881(10)	0.1254(8)	0.009(3)	O5W	0.896(2)	0.020(2)	0.5721(13)	0.040(6)
O14	0.5439(14)	0.3832(10)	0.0012(8)	0.008(3)	O6W	0.569(2)	−0.0380(14)	0.3179(11)	0.029(5)
O15	0.763(2)	0.3389(11)	0.0052(8)	0.012(4)	O7W	0.412(2)	0.097(2)	0.3475(14)	0.050(7)
O16	0.9039(14)	0.1719(10)	0.1420(8)	0.007(3)	O8W	0.271(2)	−0.067(2)	0.3534(14)	0.050(7)
O17	0.7766(14)	0.1081(10)	0.2234(8)	0.011(3)	O9W	0.659(3)	0.094(2)	0.453(2)	0.081(11)
O18	0.4431(14)	0.1801(11)	0.2122(8)	0.011(4)	O10W	0.998(3)	0.668(2)	−0.093(2)	0.071(9)
O19	0.4813(13)	0.1720(9)	0.0939(7)	0.002(3)	O11W	0.063(5)	0.047(4)	0.237(3)	0.14(2)
O20	0.6005(13)	0.2300(10)	0.0178(8)	0.004(3)					

[a] Asterisks denote atoms refined anisotropically. $U_{eq} = (4/3)[a^2B(1,1) + b^2B(2,2) + c^2B(3,3) + ab(\cos\gamma)B(1,2) + ac(\cos\beta)B(1,3) + bc(\cos\alpha)B(2,3)]$.

Scheme 1. Synthetic Routes to the **Ni$_3$**, **Ni$_4$**, and **Ni$_9$** Clusters

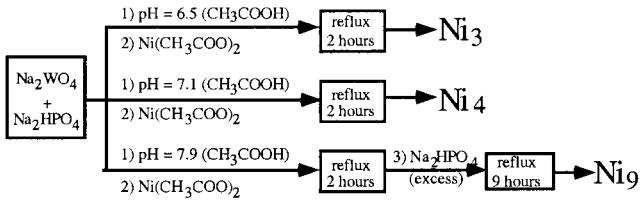

to cations (K^+ and Na^+) and water molecules. In **Ni$_4$** almost all the water molecules expected from the thermal analysis were found, without disorder. However, in **Ni$_9$** only half of the water molecules were successfully found (thermal analysis indicates the presence of 52 molecules of water), and one Na^+ cation was disordered over two different positions. The large number of peaks and the disorder made difficult the final assignment to distinguish between Na^+ atoms or water molecules, and in all cases criteria about the height of the peak and its first coordination sphere (being the cations surrounded by water molecules) were applied. Nevertheless, no further modelization of this was required since the anions, which did not appear to be affected by disorder, were already clear when convergence was reached at the *R* values given in Table 1. This *R* value is somewhat high, but is low if compared with that obtained for the analogous Co cluster, as reported by Weakley. This high value could be related to the loss of some zeolitic water from the crystal during transit, with enhancement of the disorder for the remaining water molecules. No hydrogen atoms were included in the structural model. Only heavy atoms were refined anisotropically in both cases.

Magnetic Properties. Variable temperature susceptibility measurements were carried out in the temperature range 2−300 K at a magnetic field of 0.1 T on polycrystalline samples with a magnetometer (Quantum Design MPMS-XL-5) equipped with a SQUID sensor. The susceptibility data were corrected from the diamagnetic contributions of the polyanions as deduced by using Pascal's constant tables.

Results and Discussion

Synthesis. Polyoxometalate coordination chemistry is often dominated by a large number of equilibria among different species, all of them present in solution. This feature difficults the selective isolation of a given complex in the solid state. In our effort of preparing the Ni analogue to the tetranuclear cluster series M_4 (not yet reported to our knowledge), we confronted all these problems of equilibria in solution carrying out a deeper study of the reaction conditions.[18] This study allowed us to obtain in a controlled manner three different complexes of increasing nickel nuclearities (from 3 to 9). Although none of the products is obtained exclusively, we found the best conditions to obtain in high yield the desired nickel complex. The factors that affect these equilibria are mainly pH and temperature, and, to a lesser extent, the concentration of reagents. The general synthetic procedure is summarized in Scheme 1. Different pH conditions were tried between 6 and 8, since at lower pH the predominant polyoxotungstate species is the monovacant $[PW_{11}O_{39}]^{7-}$, and so the $[Ni(H_2O)PW_{11}O_{39}]^{5-}$ structure is favored, while at higher pH the basic hydrolysis of the polyoxometalates occurs. The observed pattern indicated that at higher pH or higher temperatures, the equilibria are displaced to the higher nuclearities. So, by slight variation of the pH of an aqueous solution containing tungstate and phosphate (proportion 9:1) and Ni^{II}, salts of the different polyoxoanion complexes are isolated by addition of K^+: at pH = 6.3, pale green needles of the **Ni$_3$** complex are mainly obtained; at pH = 6.9, the **Ni$_4$** complex, obtained as chunky yellow prisms, is the main product; finally, at pH = 7.5, **Ni$_9$** is isolated predominantly, as emerald

(18) In fact, following the general synthetic method proposed for the M_4 series yielded, in the case of Ni, the anion $[Ni_3(H_2O)_3(PW_{10}O_{39})H_2O]^{7-}$.

Table 3. Atom Coordinates and Thermal Isotropic or Equivalent Isotropic Parameters for $H_{121}K_5Na_{11}Ni_9O_{171}P_5W_{27}$ (**Ni_9**)[a]

atom	*x*	*y*	*z*	*U* (Å^2)	atom	*x*	*y*	*z*	*U* (Å^2)
W1	0.4766(2)	0.0605(4)	0.8179(2)	0.0474(13)*	O40	0.419(4)	0.321(9)	0.776(3)	0.07(3)
W2	0.5305(2)	0.3253(4)	0.8426(2)	0.050(2)*	O41	0.455(5)	0.527(12)	0.833(4)	0.08(4)
W3	0.5218(2)	0.1283(5)	0.9112(2)	0.051(2)*	O42	0.492(4)	0.426(8)	0.920(3)	0.06(2)
W4	0.3805(2)	0.1891(4)	0.7733(2)	0.0430(12)*	O43	0.447(3)	0.187(7)	0.963(2)	0.05(2)
W5	0.4338(2)	0.4480(4)	0.7972(2)	0.0452(12)*	O44	0.402(2)	−0.004(5)	0.881(2)	0.045(12)
W6	0.4739(2)	0.5116(4)	0.8827(2)	0.0466(13)*	O45	0.358(4)	0.044(10)	0.788(4)	0.06(3)
W7	0.4659(2)	0.3176(4)	0.9498(2)	0.0450(13)*	O46	0.377(2)	0.313(4)	0.864(14)	0.022(10)
W8	0.4169(2)	0.0750(4)	0.9275(2)	0.0440(13)*	O47	0.341(3)	0.273(7)	0.791(2)	0.07(2)
W9	0.3735(2)	0.0088(4)	0.8368(2)	0.0400(12)*	O48	0.386(2)	0.460(5)	0.814(2)	0.027(12)
W10	0.0681(2)	0.6171(5)	0.6660(2)	0.0749(14)*	O49	0.423(3)	0.525(6)	0.891(2)	0.03(2)
W11	0.1277(2)	0.8737(4)	0.6887(2)	0.0451(13)*	O50	0.406(4)	0.376(8)	0.940(3)	0.06(3)
W12	0.1685(2)	0.6818(5)	0.63108(14)	0.0447(12)*	O51	0.366(3)	0.136(6)	0.915(2)	0.06(2)
W13	0.0815(2)	0.5607(5)	0.7529(2)	0.0467(13)*	O52	0.337(6)	0.077(14)	0.845(5)	0.11(5)
W14	0.1405(2)	0.8128(4)	0.7760(2)	0.0449(13)*	O53	0.084(3)	0.768(6)	0.680(2)	0.03(2)
W15	0.2330(2)	0.8705(4)	0.7432(2)	0.0422(12)*	O54	0.114(2)	0.616(4)	0.6408(14)	0.018(10)
W16	0.2727(2)	0.6777(5)	0.6868(2)	0.0435(12)*	O55	0.160(3)	0.806(6)	0.655(2)	0.03(2)
W17	0.2157(2)	0.4420(5)	0.6650(2)	0.0452(13)*	O56	0.133(3)	0.558(7)	0.718(3)	0.06(2)
W18	0.1185(2)	0.3811(4)	0.7005(2)	0.0460(12)*	O57	0.173(3)	0.748(6)	0.732(2)	0.04(2)
W19	0.1434(2)	0.2982(5)	1.0159(2)	0.0455(13)*	O58	0.201(5)	0.605(11)	0.691(4)	0.09(4)
W20	0.2022(2)	0.5541(5)	1.04303(14)	0.0429(12)*	O59	0.044(4)	0.597(8)	0.706(3)	0.02(3)
W21	0.0845(2)	0.5574(5)	0.9920(2)	0.0475(13)*	O60	0.110(3)	0.865(6)	0.728(2)	0.06(2)
W22	0.2279(2)	0.2290(4)	0.9748(2)	0.0417(12)*	O61	0.179(4)	0.926(10)	0.705(4)	0.10(3)
W23	0.2864(2)	0.4790(5)	1.00224(14)	0.0411(12)*	O62	0.230(5)	0.716(12)	0.641(4)	0.01(4)
W24	0.2325(2)	0.7181(5)	0.98168(14)	0.0450(13)*	O63	0.182(3)	0.538(8)	0.630(3)	0.07(2)
W25	0.1174(2)	0.7193(4)	0.9312(2)	0.0436(12)*	O64	0.079(2)	0.473(4)	0.668(14)	0.020(9)
W26	0.0632(2)	0.4842(4)	0.9053(2)	0.0418(12)*	O65	0.094(2)	0.718(5)	0.763(2)	0.057(14)
W27	0.1198(2)	0.2304(4)	0.92868(14)	0.0433(12)*	O66	0.192(2)	0.891(5)	0.775(2)	0.030(12)
Ni1	0.3272(5)	0.383(2)	0.8187(4)	0.032(4)*	O67	0.255(3)	0.807(7)	0.705(3)	0.06(2)
Ni2	0.3662(5)	0.4376(14)	0.8992(5)	0.041(4)*	O68	0.266(6)	0.543(14)	0.671(5)	0.08(6)
Ni3	0.3222(6)	0.218(2)	0.8773(5)	0.038(4)*	O69	0.157(3)	0.408(6)	0.671(2)	0.04(2)
Ni4	0.1944(6)	0.5596(13)	0.8064(5)	0.044(4)*	O70	0.077(4)	0.427(9)	0.726(3)	0.08(3)
Ni5	0.2786(5)	0.6170(12)	0.7769(4)	0.036(3)*	O71	0.214(2)	0.564(5)	0.756(2)	0.034(12)
Ni6	0.2276(6)	0.3979(14)	0.7570(5)	0.044(4)*	O72	0.129(3)	0.527(6)	0.785(2)	0.06(2)
Ni7	0.2578(5)	0.4103(13)	0.9113(4)	0.039(4)*	O73	0.177(4)	0.719(8)	0.802(3)	0.07(2)
Ni8	0.2071(6)	0.6288(13)	0.8932(4)	0.040(4)*	O74	0.258(3)	0.777(6)	0.770(2)	0.03(2)
Ni9	0.1570(5)	0.4103(14)	0.8694(5)	0.043(4)*	O75	0.295(2)	0.637(5)	0.729(2)	0.029(11)
P1	0.422(2)	0.264(4)	0.8612(13)	0.056(12)*	O76	0.236(3)	0.410(6)	0.708(2)	0.04(2)
P2	0.1804(13)	0.619(3)	0.7213(9)	0.028(9)*	O77	0.164(3)	0.365(6)	0.731(2)	0.06(2)
P3	0.1751(12)	0.476(3)	0.9533(9)	0.027(8)*	O78	0.185(4)	0.404(10)	1.034(3)	0.03(3)
P4	0.2915(10)	0.586(2)	0.8609(8)	0.050(6)*	O79	0.098(3)	0.402(6)	1.004(2)	0.04(2)
P5	0.2274(10)	0.315(3)	0.8306(10)	0.033(7)*	O80	0.141(3)	0.585(7)	1.020(3)	0.06(2)
O1	0.493(8)	−0.01(2)	0.794(7)	0.17(8)	O81	0.168(2)	0.354(5)	0.964(2)	0.011(13)
O2	0.580(3)	0.335(6)	0.830(2)	0.03(2)	O82	0.210(3)	0.535(7)	0.984(2)	0.04(2)
O3	0.572(4)	0.048(10)	0.921(3)	0.05(3)	O83	0.135(3)	0.532(7)	0.949(3)	0.05(2)
O4	0.358(2)	0.189(5)	0.733(2)	0.046(14)	O84	0.196(4)	0.225(10)	1.006(4)	0.06(3)
O5	0.431(5)	0.538(10)	0.760(4)	0.10(3)	O85	0.263(2)	0.504(5)	1.044(2)	0.026(12)
O6	0.499(3)	0.626(7)	0.901(2)	0.08(2)	O86	0.214(3)	0.680(8)	1.023(3)	0.03(2)
O7	0.485(4)	0.363(9)	0.987(3)	0.04(3)	O87	0.085(6)	0.677(13)	0.967(5)	0.08(5)
O8	0.407(6)	−0.019(14)	0.959(5)	0.06(6)	O88	0.051(3)	0.523(6)	0.947(2)	0.05(2)
O9	0.342(3)	−0.116(6)	0.831(2)	0.04(2)	O89	0.108(3)	0.209(8)	0.978(3)	0.05(2)
O10	0.016(3)	0.645(6)	0.635(2)	0.06(2)	O90	0.262(3)	0.330(7)	1.003(2)	0.02(2)
O11	0.095(4)	0.975(10)	0.670(3)	0.057(3)	O91	0.280(4)	0.630(9)	1.005(3)	0.07(3)
O12	0.151(4)	0.699(9)	0.591(3)	0.06(3)	O92	0.174(3)	0.742(6)	0.963(2)	0.04(2)
O13	0.041(3)	0.559(7)	0.773(2)	0.05(2)	O93	0.069(3)	0.654(7)	0.901(2)	0.03(2)
O14	0.118(5)	0.895(10)	0.802(4)	0.08(3)	O94	0.074(3)	0.341(7)	0.920(3)	0.05(2)
O15	0.263(3)	0.967(7)	0.751(3)	0.06(2)	O95	0.173(4)	0.167(9)	0.951(3)	0.02(3)
O16	0.315(4)	0.713(9)	0.674(3)	0.09(3)	O96	0.192(4)	0.483(8)	0.918(3)	0.06(2)
O17	0.231(6)	0.339(13)	0.641(5)	0.16(5)	O97	0.246(3)	0.272(6)	0.936(2)	0.03(2)
O18	0.103(5)	0.275(12)	0.687(4)	0.12(4)	O98	0.285(4)	0.472(8)	0.955(3)	0.05(3)
O19	0.129(6)	0.249(13)	1.041(5)	0.15(5)	O99	0.239(3)	0.693(7)	0.938(2)	0.05(2)
O20	0.207(3)	0.584(6)	1.086(2)	0.04(2)	O100	0.1512(2)	0.708(5)	0.904(2)	0.033(13)
O21	0.048(4)	0.559(10)	1.013(4)	0.07(3)	O101	0.096(3)	0.475(7)	0.876(2)	0.04(2)
O22	0.263(4)	0.133(9)	0.987(3)	0.07(3)	O102	0.141(4)	0.268(9)	0.891(3)	0.05(3)
O23	0.347(5)	0.465(12)	1.023(4)	0.09(4)	O103	0.290(3)	0.461(6)	0.780(2)	0.03(2)
O24	0.252(3)	0.846(7)	0.987(3)	0.02(2)	O104	0.173(2)	0.553(5)	0.850(2)	0.024(13)
O25	0.094(2)	0.838(4)	0.921(2)	0.040(11)	O105	0.313(2)	0.347(5)	0.905(2)	0.029(11)
O26	0.009(4)	0.455(9)	0.877(3)	0.08(3)	O106	0.319(3)	0.485(7)	0.850(3)	0.06(2)
O27	0.091(4)	0.138(9)	0.912(3)	0.07(3)	O107	0.284(4)	0.301(8)	0.838(3)	0.03(2)
O28	0.504(4)	0.202(8)	0.820(3)	0.06(2)	O108	0.265(4)	0.609(9)	0.826(3)	0.03(3)
O29	0.493(4)	0.054(9)	0.864(3)	0.05(3)	O109	0.220(5)	0.400(11)	0.803(4)	0.06(4)
O30	0.541(3)	0.228(8)	0.882(3)	0.08(2)	O110	0.263(3)	0.556(7)	0.884(2)	0.04(2)
O31	0.418(3)	0.163(8)	0.833(3)	0.03(2)	O111	0.225(5)	0.364(11)	0.868(4)	0.13(4)
O32	0.444(5)	0.341(11)	0.853(4)	0.06(3)	O112	0.352(4)	0.563(9)	0.927(3)	0.06(3)
O33	0.446(3)	0.214(8)	0.895(3)	0.030(2)	O113	0.270(3)	0.137(6)	0.892(2)	0.04(2)
O34	0.441(3)	0.103(8)	0.780(3)	0.08(2)	O114	0.343(3)	0.665(7)	0.804(2)	0.05(2)
O35	0.499(4)	0.395(8)	0.804(3)	0.07(3)	O115	0.251(3)	0.238(6)	0.762(2)	0.05(2)
O36	0.530(3)	0.440(7)	0.871(2)	0.07(2)	O116	0.215(4)	0.759(8)	0.865(3)	0.07(2)
O37	0.515(3)	0.230(7)	0.940(2)	0.07(2)	O117	0.130(2)	0.346(5)	0.822(2)	0.025(13)
O38	0.476(2)	0.034(4)	0.930(2)	0.029(10)	O118	0.317(3)	0.686(6)	0.868(2)	0.02(2)
O39	0.426(5)	−0.024(11)	0.818(3)	0.08(4)	O119	0.203(3)	0.214(6)	0.816(2)	0.026(2)

Table 3. (continued)

atom	*x*	*y*	*z*	*U* (Å^2)	atom	*x*	*y*	*z*	*U* (Å^2)
K1	0.1408(13)	0.827(3)	0.0228(11)	0.065(9)	OW5	0.018(5)	0.832(11)	0.326(4)	0.14(4)
K2	0.4775(14)	0.650(3)	0.3879(11)	0.062(9)	OW6	−0.044(4)	0.171(8)	0.412(3)	0.02(3)
K3	0.0183(13)	0.203(3)	0.4687(11)	0.076(9)	OW7	0.465(5)	0.761(12)	0.316(4)	0.13(4)
K4	0.3120(11)	0.496(3)	0.4516(9)	0.078(7)	OW8	0.362(5)	0.527(12)	0.189(4)	0.10(4)
K5	0.2756(11)	−0.006(3)	0.0460(9)	0.073(7)	OW9	0.039(6)	0.237(14)	0.335(5)	0.12(5)
Na1	0.413(2)	0.606(4)	0.063(2)	0.057(12)	OW10	0.382(6)	0.758(14)	0.231(5)	0.16(6)
Na2	0.275(2)	0.678(5)	0.338(2)	0.08(2)	OW11	0.156(4)	0.392(9)	0.264(3)	0.06(3)
Na3	0.358(3)	0.800(7)	0.117(2)	0.08(2)	OW12	0.017(5)	0.647(11)	0.217(4)	0.11(4)
Na4	0.091(3)	0.551(7)	0.360(3)	0.102(2)	OW13	0.420(6)	0.548(13)	0.001(5)	0.13(5)
Na5	0.190(2)	0.345(5)	0.208(2)	0.06(14)	OW14	0.181(5)	0.378(11)	0.372(4)	0.072(4)
Na6	0.250(3)	0.555(6)	0.152(2)	0.08(2)	OW15	0.191(6)	1.026(1)	0.059(5)	0.07(5)
Na7	0.438(3)	0.867(8)	0.459(3)	0.11(3)	OW16	0.061(5)	0.4045(11)	0.228(4)	0.12(4)
Na8	0.489(2)	0.226(5)	0.237(2)	0.09(2)	OW17	0.576(6)	0.664(14)	0.383(5)	0.14(5)
Na9	0.350(2)	0.655(5)	0.256(2)	0.065(14)	OW18	0.366(6)	0.460(13)	0.518(5)	0.09(5)
Na10	0.109(2)	0.558(5)	0.091(2)	0.07(2)	OW19	0.578(4)	0.732(10)	0.420(4)	0.07(3)
Na11†	0.336(4)	0.090(10)	0.208(3)	0.09(3)	OW20	0.199(8)	0.57(2)	0.398(6)	0.17(7)
Na12†	0.047(4)	0.344(9)	0.133(3)	0.06(3)	OW21	0.323(9)	0.02(2)	0.107(7)	0.13(9)
OW1	0.265(5)	0.794(12)	0.081(4)	0.11(4)	OW22	0.161(6)	0.975(14)	−0.011(5)	0.10(6)
OW2	0.404(4)	0.754(8)	0.401(3)	0.05(2)	OW23	0.091(6)	0.10(2)	0.098(5)	0.17(6)
OW3	0.260(4)	0.514(10)	0.334(3)	0.08(3)	OW24	0.370(5)	0.231(12)	0.479(4)	0.11(4)
OW4	0.314(5)	0.703(10)	0.428(4)	0.09(3)					

[a] Asterisks denote atoms refined anisotropically: $U_{eq} = (4/3)[a^2B(1,1) + b^2B(2,2) + c^2B(3,3) + ab(\cos\gamma)B(1,2) + ac(\cos\beta)B(1,3) + bc(\cos\alpha)B(2,3)]$. Daggers denote disordered atoms with multiplicity = 0.5.

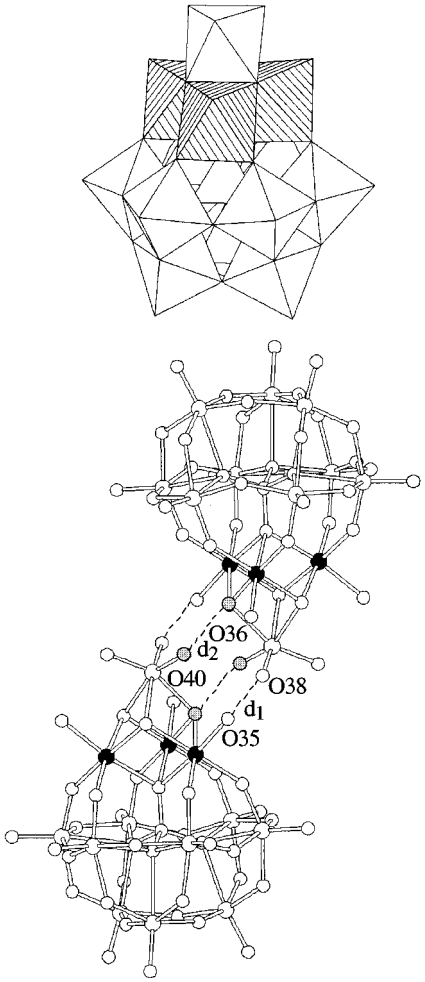

Figure 1. Polyhedral and ball-and-stick representations of the complex $[Ni_3(H_2O)_3(PW_{10}O_{39})H_2O]^{7-}$ showing the **Ni_3** cluster (shaded and in black) and the packing of the $[Ni_3(H_2O)_3(PW_{10}O_{39})H_2O]^{7-}$ complexes with the closest intercluster O−O distances.

green needles. The use of reflux increases the yields of **Ni_4** and **Ni_9**. On the other hand, the use of stoichiometric amounts of Ni^{II} does not have a big influence on the final compounds. Surprisingly enough, the addition of a big excess of Ni^{II} to the solution favors the formation of the tetranuclear cluster, although among the three complexes this is the one with less proportion of Ni in its formula. Single crystals of good quality for X-ray diffraction analysis were obtained in all the cases from recrystallization of the products in hot water.

Chart 1. Connectivity Diagram for the $[Ni_3(H_2O)_3PW_{10}O_{39}H_2O]$ (**Ni_3**) Cluster

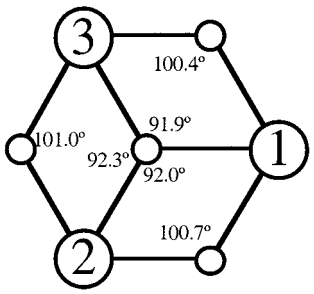

distances (Å):

d(1-2) = 3.178 d(2-3) = 3.177 d(1-3) = 3.172

Structures. Ni_3 exhibits a unique structure, found only for nickel, that contains a triangular Ni_3O_{13} unit, formed by three edge-sharing NiO_6 octahedra with the Ni^{II} ions coordinated by the ligand $(PW_9O_{34})^{9-}$ (α-B isomer) and a WO_6 octahedron (Figure 1). This polyoxoanion may be viewed as a reconstituted Keggin-like structure $\{PNi_3W_9O_{40}\}$ with an additional cap of tungsten forming a distorted $[Ni_3WO_4]$ cubane-type core with the triangular Ni_3O_{12} entity. Each NiO_6 octahedron is formed by four oxide ions, a bridging oxygen from the central phosphate group, and a terminal oxygen from a coordinated water molecule. This gives an overall charge for the polyanion of −7. The relevant Ni−Ni distances and Ni−O−Ni angles are summarized in Chart 1. In the solid state these polyoxoanions are associated pairwise by hydrogen bonds via the coordinated water molecules O40 and O35 (Figure 1; d_1 = 2.68 Å, d_2 = 2.73 Å), in such a way that the triangular Ni_3O_{12} units are parallel and well-isolated magnetically.

Ni_4 has the well-known M_4 structure already reported for M = Co, Zn, Cu, and Mn: two ligands $(PW_9O_{34})^{9-}$ are encapsulating a centrosymmetric rhomb-like Ni_4O_{16} unit, formed by four edge-sharing NiO_6 octahedra (Figure 2). The relevant Ni−Ni

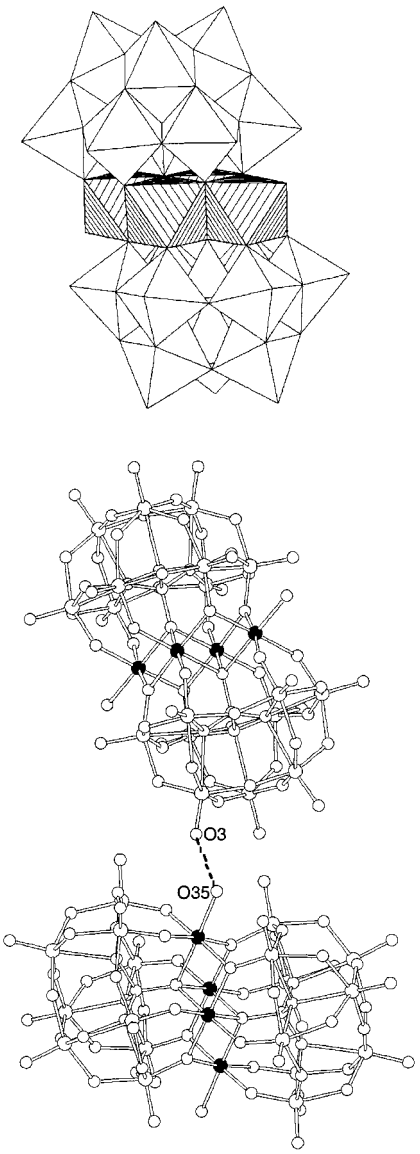

Figure 2. Polyhedral and ball-and-stick representations of the complex $[Ni_4(H_2O)_2(PW_9O_{34})_2]^{10-}$ showing the **Ni_4** cluster (shaded and in black) and the packing of the $[Ni_4(H_2O)_2(PW_9O_{34})_2]^{10-}$ complexes with the closest intercluster O−O distances.

Chart 2. Connectivity Diagram for the $[Ni_4(PW_9O_{34})_2(H_2O)_2]$ (**Ni_4**) Cluster

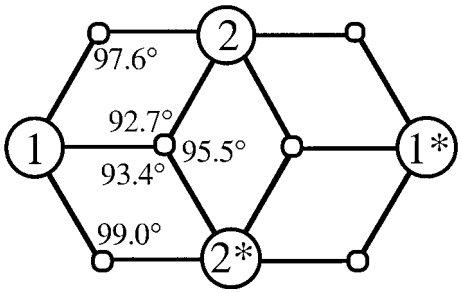

distances (Å):

d(1-2) = 3.124 d(1-2*) = 3.109

d(2-2*) = 3.196 d(1-1*) = 5.352

distances and Ni−O−Ni angles are summarized in Chart 2. As far as the crystal structure is concerned, we notice that the Ni salt crystallizes in a different way to the previous related

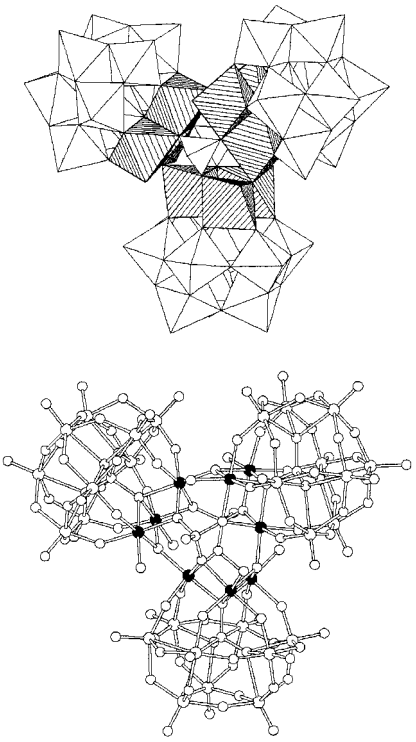

Figure 3. Polyhedral and ball-and-stick representations of the complex $[Ni_9(OH)_3(H_2O)_6(HPO_4)_2(PW_9O_{34})_3]^{16-}$ showing the **Ni_9** cluster (shaded and in black).

Chart 3. Connectivity Diagram for the $[Ni_9(OH)_3(H_2O)_6(HPO_4)_2(PW_9O_{34})_3]$ (**Ni_9**) Cluster

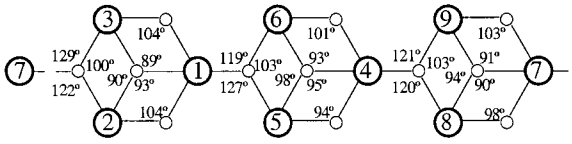

distances (Å):

d(1-2) = 3.18; d(1-3) = 3.16; d(2-3) = 3.09
d(1-5) = 3.49; d(1-6) = 3.47; d(5-6) = 3.13
d(4-5) = 3.16; d(4-6) = 3.15; d(4-8) = 3.44
d(4-9) = 3.49; d(8-9) = 3.13; d(7-8) = 3.11
d(7-9) = 3.11; d(2-7) = 3.48; d(3-7) = 3.53

analogues,[6] although in the same space group (monoclinic). In this crystal structure the polyoxoanions are packed forming layers in which every anion has close hydrogen bondings (d = 2.69 Å) via the two water molecules coordinated to the Ni^{II} ions of the long diagonal of the rhomb and one terminal oxo group coordinated to a tungsten atom (Figure 2). The tetranuclear magnetic clusters present two different almost orthogonal orientations.

In **Ni_3** and **Ni_4**, despite the presence of hydrogen bonding, the magnetic clusters are perfectly isolated since all the hydrogen bonds are found between water molecules from the Ni coordination sphere and oxo groups linked to tungsten atoms.

Ni_9 contains a central Ni_9O_{36} cluster formed by three triangular Ni_3O_{13} edge-sharing units. These triangles are connected to each other by three OH^- bridging groups and two central HPO_4^{2-} groups in order to form a triangle of triangles (Figure 3). It is interesting to notice that, in contrast to **Ni_3**, only two of the three Ni centers have a coordinated water molecule, as the third one has an OH^- group bridging two **Ni_3** units. Still, this difference has no significant effect on the geometry of the triangle which, within the error in the X-ray structural determination, presents Ni−Ni distances and Ni−O−

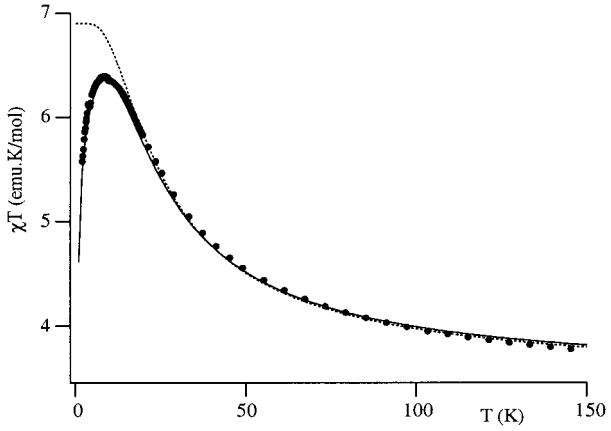

Figure 4. $\chi_m T$ product vs T for the **Ni$_3$** cluster. Solid and dotted lines represent the best fit to the anisotropic and isotropic models, respectively (see text).

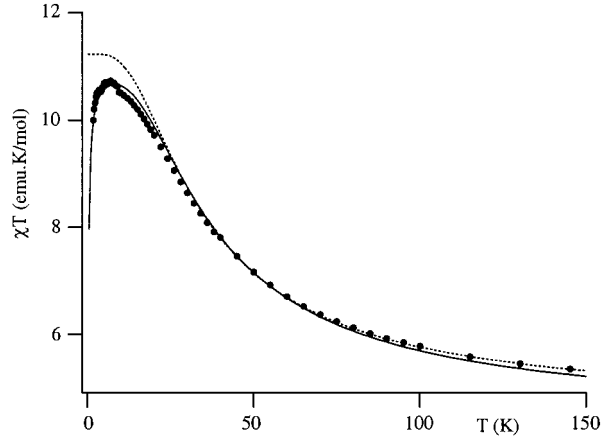

Figure 5. $\chi_m T$ product vs T for the **Ni$_4$** cluster. Solid and dotted lines represent the best fit to the anisotropic and isotropic models, respectively (see text).

Ni angles close to those observed in **Ni$_3$** (see Chart 3). The periphery of this polyoxoanion is formed by three diamagnetic ligands $(PW_9O_{34})^{9-}$ which guarantee the insulation of the magnetic clusters. These ligands are coordinating the **Ni$_3$** triangles to form a reconstituted Keggin-like structure $\{PNi_3W_9O_{40}\}$. Hence, the polyoxoanion may be viewed as resulting from the condensation of three of these Keggin units. An additional guarantee of the ideal insulation of the magnetic clusters comes from the crystal packing of these polyoxoanions which are forming centrosymmetric layers, with no hydrogen bond interactions.

Magnetic Properties. The magnetic behaviors of the three compounds are displayed as plots of the product $\chi_m T$ vs T in Figures 4, 5, and 7 for the **Ni$_3$**, **Ni$_4$**, and **Ni$_9$** clusters, respectively. In the three cases $\chi_m T$ shows an increase as the temperature is decreased. For **Ni$_3$** and **Ni$_4$** this increase is more important and is followed by a maximum corresponding to $\chi_m T = 6.3$ and 10.7 emu K mol^{-1} at $T = 8.3$ and 6.1 K, respectively; finally, a sharp decrease is observed at lower temperatures. In contrast, for **Ni$_9$** the maximum corresponding to $\chi_m T = 14.2$ emu K mol^{-1}, occurs at higher temperatures (25 K).

The magnetic properties of these clusters are largely due to interactions between $^3A_2$ nickel(II) ions. The exchange pathways connecting the nickel(II) ions can be schematized as shown in Chart 4. In **Ni$_3$** and **Ni$_4$** the Ni−Ni pairwise interactions between the spins $S = 1$ are exclusively transmitted through the oxo bridges. In view of the geometry of these clusters and, in particular, of the Ni−O−Ni angles, ferromagnetic exchange interactions are expected to occur in these two systems. In fact, all these angles are comprised between 90° and 100°, which are in the range where the Ni−Ni ferromagnetic exchange

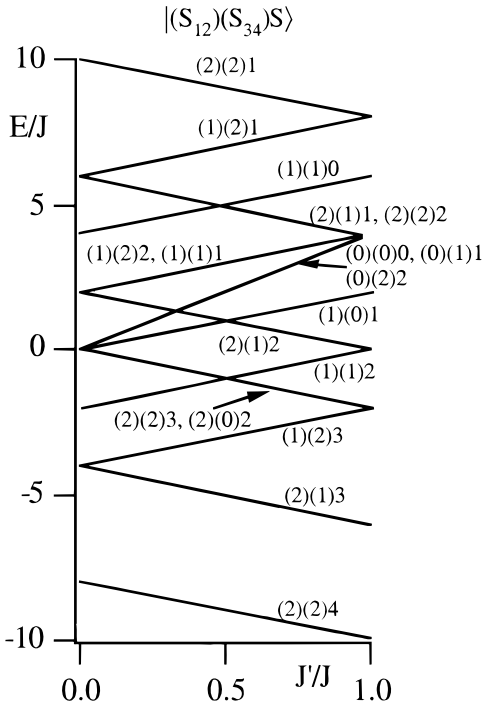

Figure 6. Energy levels of the **Ni$_4$** cluster as a function of the J'/J ratio. The wave functions are labeled according to the Kambe-type coupling scheme (S_{12} and S_{34} are intermediate spin values, and S is the total spin).

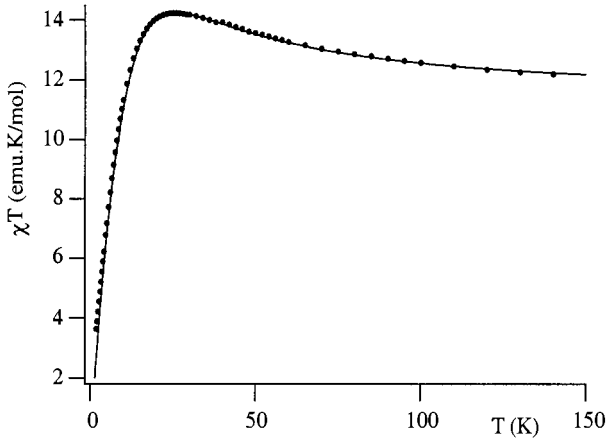

Figure 7. $\chi_m T$ product vs T for the **Ni$_9$** cluster. The solid line represents the best fit to the isotropic model (see text).

Chart 4. Exchange Pathways for the **Ni$_3$**, **Ni$_4$**, and **Ni$_9$** Clusters

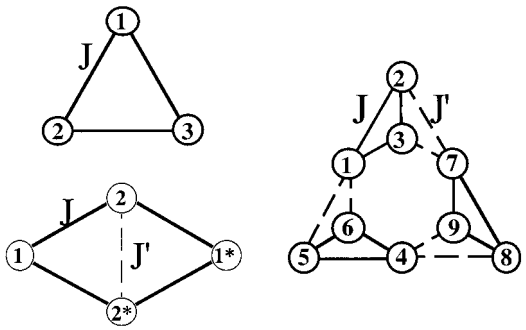

pathways are dominant (90 ± 14°).[19] The steady increase in $\chi_m T$ on decreasing temperature confirms this point, thus indicating that ground spin states of these clusters are 3 and 4, respectively. Accordingly, these clusters are EPR silent at low frequencies (X band).

In **Ni$_9$** the exchange pathways are more complex than in the previous cases as they involve not only the oxo bridges but also the two central HPO_4^{2-} groups. Still, the ability of this group to propagate exchange interactions is small compared to that of the μ-oxo groups. Then, to reduce the number of exchange parameters such pathways have been omitted in the exchange network shown in Chart 4. This scheme considers two kinds of exchange interactions: the intra-triangle exchange, J, associated to the Ni−Ni interactions within the **Ni$_3$** edge-sharing clusters from each Keggin subunit, and the inter-triangle exchange, J', that accounts for the Ni−O−Ni connections between different **Ni$_3$** triangles. As this last involves corner-sharing NiO_6 octahedra with Ni−O−Ni angles around 120° or even larger, this exchange pathway should be antiferromagnetic. Therefore, an unprecedented nickel cluster with coexistence of both ferro- and antiferromagnetic couplings is to be expected. The magnetic properties confirm this prediction: the increase in $\chi_m T$ down to 25 K indicates the presence of dominant ferromagnetic interactions within the triangles, while the sharp decrease at lower temperatures is a consequence of the antiferromagnetic inter-triangle interactions.

Analysis of the Magnetic Properties. The theoretical calculation of the thermally accessible energy levels and of the magnetic properties of large clusters requires the use of an efficient computational approach. Only in some simple cases, calculations of the spin levels can be performed using the well-known Kambe's method.[20] This method works when the exchange Hamiltonian is fully isotropic (Heisenberg model) and can be expressed through an appropriate set of intermediate spin operators that directly gives a diagonal eigenmatrix. Unfortunately, this method is restricted to simple cases with high symmetry. Thus, even for the calculation of a fully distorted triangle, this procedure becomes cumbersome. In the case of high-nuclearity clusters an efficient procedure has been developed by Gatteschi et al.[21] using irreducible tensor operators (ITO) and point symmetry classification of the functions. This procedure is restricted to magnetic clusters formed by a finite assembly of identical spins coupled by isotropic interactions. To consider also the anisotropic terms of the electronic Hamiltonian (anisotropic and antisymmetric exchanges, single ion anisotropy), and the possibility of having different local spins, we have developed a more general procedure that expresses these anisotropic terms in terms of complex ITOs.[22] This approach is supported by an efficient computing program[23] that allows to treat spin clusters formed by an arbitrary number of magnetic sites, N, with spins S_1, S_2, ..., S_N, where each local spin S_i can have a different value. The procedure has three subsequent steps. In the first step the basis set of spin functions is obtained by a successive spin coupling scheme ($S_1 + S_2 = \tilde{S}_2$, $\tilde{S}_2 + S_3 = \tilde{S}_3$, ..., $\tilde{S}_{N-1} + S_N = S$, where $\tilde{S}_2 = S_{12}$, $\tilde{S}_3 = S_{123}$, etc. are the intermediate spin values, and S is the full spin). In a second step the matrix element of each term of the Hamiltonian (isotropic or anisotropic) is expressed in terms of complex ITOs. In a third step the decoupling of these ITOs allows to express the matrix elements in terms of the spin operators acting on the individual spin space of each center, and of the well-known recoupling coefficients, 9j-symbols.[24]

Table 4. Magnetic Parameters of the **Ni$_3$**, **N$_4$**, and **Ni$_9$** Clusters

cluster	J (cm^{-1})	J' (cm^{-1})	D (cm^{-1})	g
Ni$_3$O$_{13}$	3.9		5.8	$g_\parallel = 2.5$; $g_\perp = 2$
Ni$_4$O$_{16}$	6.5	2.5	4.5	$\bar{g} = 2.12$
Ni$_9$O$_{36}$	3.9	−1.4		$\bar{g} = 2.24$

A preliminary analysis of the magnetic behaviors of **Ni$_3$** and **Ni$_4$** has been done by assuming an isotropic Heisenberg exchange Hamiltonian, as in this way analytical expressions for the eigenvalues and susceptibilities are easily derived from the vector coupling method of Kambé.[25] We observe that the isotropic exchange model provides a good description of the magnetic data for temperatures above the maximum in $\chi_m T$ (dotted lines in Figures 4 and 5). However, at lower temperatures the model predicts a plateau corresponding to the ground spin state of the cluster ($S = 3$ and 4, for **Ni$_3$** and **Ni$_4$**), while the magnetic data show a maximum followed by a decrease in $\chi_m T$ which has its origin in the zero-field splitting of the local nickel(II) spins, as the intercluster antiferromagnetic interactions are expected to have a quite negligible effect, due to the good insulation of the magnetic clusters in the structure. Thus, a more rigorous treatment is required that considers both isotropic exchange interactions and an axial single ion anisotropy of the type DS_{iz}^2, where D represents the zero-field splitting parameter. The numerical procedure described above has allowed us to take this effect into account. An excellent agreement with the experiment has been obtained in the case of **Ni$_3$** (Figure 4) with the set of parameters reported in Table 4. In the case of **Ni$_4$**, however, several sets of parameters can be used to fit in a satisfactory manner the experimental data with J' between 0 and 5 cm^{-1}, while J remains within the range 6.2−7.0 cm^{-1} (Figure 5). This insensitivity of the magnetic properties to J' is a consequence of the topology of the cluster which leads to an energy spectrum where the energy gap between the ground spin level ($S = 4$) and the first excited one ($S = 3$) is equal to $4J$, being independent on J' (Figure 6). In fact, the magnetic properties have shown to be largely insensitive to J'. To account for the single-ion ZFS of the two Ni(II) sites, an averaged D value has been introduced in the fitting. To get a more accurate determination of the magnetic parameters of this cluster (in particular of J' and D) spectroscopic measurements such as inelastic neutron scattering and high-field EPR spectra are being performed and will be published elsewhere.

Finally, for the quantitative analysis of the magnetic properties of **Ni$_9$** we have also used the numerical procedure. In this system the size of the problem (the overall states to be considered are $3^9 = 19\,683$) has imposed the use of a fully isotropic Hamiltonian, neglecting thus the single-ion anisotropy effects. Still these effects are somewhat accounted by the intertriangular magnetic exchange, J', which is antiferromagnetic. A good reproduction of the experiment is obtained when a dominant ferromagnetic exchange within the triangles coexist with a

(19) Bertrand, J. A.; Ginsberg, A. P.; Kaplan, R. I.; Kirkwood, C. E.; Martin, R. L.; Sherwood, R. C. *Inorg. Chem.* **1971**, *10*, 240.
(20) Hatfield, W. E. *Theory and Applications of Molecular Paramagnetism*; Wiley: New York, 1976.
(21) Gatteschi, D.; Pardi, L. *Gazz. Chim. Ital.* **1993**, *123*, 231.
(22) Clemente, J. M.; Palii, A. V.; Tsukerblat, B. S.; Georges, R. In *Molecular Magnetism: From Molecular Assemblies to the Devices*; Coronado, E., Delhaes, P., Gatteschi, D., Miller, J. S., Eds.; NATO ASI Series E321; Kluwer Academic Publishers: Dordrecht, The Netherlands, 1996; p 85.
(23) Clemente, J. M. Ph.D. Thesis, University of Valencia, 1998.
(24) Varshalovich, D. A.; Moskalev, A. N.; Khersonskii, V. K. *Quantum Theory of Angular Momentum*; World Scientific Publishing: Singapore, 1988.
(25) Gladfelter, W. L.; Lynch, M. W.; Schaefer, W. P.; Hendrickson, D. N.; Gray, H. B. *Inorg. Chem.* **1981**, *20*, 2390.

weaker antiferromagnetic exchange between the triangles (Figure 7 and Table 4). This leads to the stabilization of the lower spin states in such a way that the $S = 0$ spin state becomes the ground state of the **Ni$_9$** cluster. An interesting result of this analysis is that the intratriangle exchange parameter obtained in this large magnetic cluster compares quite well with those obtained from the analysis of the simpler clusters ($J = 3.9$, 6.8, and 3.9 cm^{-1} in **Ni$_3$**, **Ni$_4$**, and **Ni$_9$**, respectively). This confirms the validity of the models and of the magneto-structural correlations in these Ni clusters.

Conclusion

In this work we have reported three novel magnetic clusters of nickel(II) obtained by using the B-$[PW_9O_{34}]^{9-}$ ligand. Three main points must be emphasized:

(i) From the chemical point of view, we have illustrated how polyoxometalate chemistry allows to increase the number of exchange coupled magnetic centers from 3 to 9 using preformed building blocks. A remarkable result has been the preparation in good yields (∼30%) of the large polyoxometalate $[Ni_9(OH)_3(H_2O)_6(HPO_4)_2(PW_9O_{34})_3]^{16-}$. So far, only the analogous Co_9 cluster was known.[10] It was just identified as a minor product (∼5%) in the synthesis of Co_4. The method we have reported here is general and enables also the selective synthesis of the Co_9 cluster.

(ii) From the structural point of view, we should notice the discovery of an unprecedented polyoxometalate complex derived from the Keggin structure: the anion $[Ni_3(H_2O)_3(PW_{10}O_{39})H_2O]^{7-}$. The structure of this anion was the subject of a previous communication.[16] It is to be noticed that only the Ni(II) derivative has been prepared. Under the same conditions of synthesis, the other divalent metals (Co, Zn, Mn, and Cu) lead to the series M_4 or to the monosubstituted Keggin complexes.

(iii) From the magnetic point of view, we have shown that these polyoxometalate complexes constitute ideal models for the study of the exchange interactions in highly symmetrical clusters of increasing nuclearities and controlled magnetic couplings. Thus, the ferromagnetic interactions resulting from the presence of NiO_6 octahedra sharing edges, has led to the stabilization of the high-spin states $S = 3$ and $S = 4$ (for the clusters **Ni$_3$** and **Ni$_4$**). These values represent the highest ground spin states reported in polyoxometalate chemistry. On the other hand, in the **Ni$_9$** cluster the coexistence of NiO_6 octahedra sharing edges and corners has led to the observation for the first time of a coexistence of competing ferromagnetic and antiferromagnetic exchange interactions in the same cluster. Owing to the topology of the cluster, these antiferromagnetic interactions should give rise to spin frustration effects within the cluster.

Acknowledgment. We thank the Spanish DGICYT and CICYT for founding this work (Grant PB96-0862). J.R.G.M. and J.M.C.J. thank the Generalitat Valenciana for a predoctoral grant. We also thank the Spanish CICYT and the Generalitat Valenciana for the financial support to purchase the SQUID magnetometer.

Supporting Information Available: Listings of the anisotropic thermal parameters, selected bond lengths, and selected bond angles for **Ni$_4$** and **Ni$_9$** (16 pages). Ordering information is given on any current masthead page.

IC9807902